

Overview of the low- x experiments

Radek Žlebčík*

DESY

E-mail: radek.zlebcik@desy.de

The LHC, Tevatron and HERA experimental results are reviewed with a focus on the low- x kinematic domain where the BFKL dynamics, saturation effects and the gluon's transverse momentum play a role. In particular, the low- x DIS region, the central exclusive production in the pp and pA collisions and the forward jets produced in pp and pA are discussed.

Light Cone 2019 - QCD on the light cone: from hadrons to heavy ions - LC2019
16-20 September 2019
Ecole Polytechnique, Palaiseau, France

*Speaker.

1. Introduction

Over the decades, following progress in the accelerator science, processes at higher and higher centre-of-mass energies have been studied. It has allowed not only to probe particle productions at the high scales (the DGLAP limit) but also to probe hadron structure in the low- x region (BFKL limit), where x is the longitudinal momentum fraction of the parton with respect to the whole hadron momentum (typically to the proton). This is sometimes also called high-energy limit since high beam energies are needed to produce particles from low- x parton with scales in the perturbative QCD region (for a short review see [1]). At the low- x the parton distributions are dominated by gluon and the quark contribution below $x \lesssim 0.01$ is often neglected. The BFKL evolution equations predict gluon distribution to be steeply rising as $\approx x^{-0.5}$ when $x \rightarrow 0$. However, there are strong arguments that the PDFs cannot grow infinitely and that the number of gluons saturates [2]. The saturation effects can be described by the BK [3, 4] non-linear evolution equations or more generally by the JIMWLK.

In the high energy limit, the partonic emissions are expected to be ordered in the rapidity, rather than in transverse momentum, and the transverse momentum of the parton should play an important role (Fig. 1).

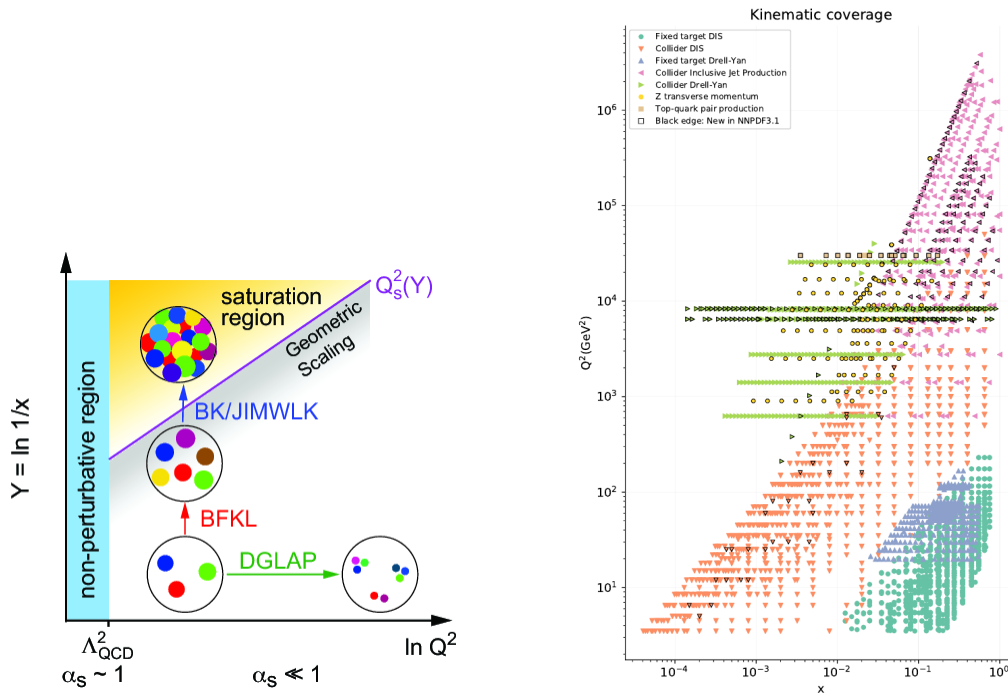


Figure 1: A diagram explaining the high-scale Q^2 and low x limits (left). The right plot shows the phase space coverage of the data points used in the NNPDF 3.1 PDF fit [5], notice that x and Q^2 axes are swapped.

In this text, we briefly review a selection of the measurements sensitive to the low- x partonic distributions. Notice, that most of them are not included in the classical global PDF fits, although they are very sensitive to the low- x gluon distribution. It could be due to significant theoretical uncertainties of the predictions (mostly only at LO pQCD) and the difficulty in treating possible

BFKL effects in the DGLAP-based fitting frameworks. For example the NNPDF 3.1 PDF fit [5] includes the HERA DIS data up to $x \sim 5 \times 10^{-5}$ and the LHC DY data up to $x \sim 2 \times 10^{-4}$ (Fig. 1).

2. Inclusive DIS at HERA

The reduced cross section σ_r , measured in the inclusive deep-inelastic ep scattering is a baseline for studies of the proton partonic structure. At the fixed centre-of-mass energy \sqrt{s} the x is from process kinematics always $x > \frac{Q^2}{s}$, consequently to reach low- x the \sqrt{s} have to be high or Q^2 low. Consequently, the low- x data points also have low Q^2 . However, since the renormalization and factorization scales are typically assigned to Q^2 , the Q^2 must be still much higher than λ_{QCD} , i.e. $\gtrsim 2 \text{ GeV}^2$ to be within pQCD regime. Really, the DGLAP QCD fits of the HERA combined legacy DIS data [6], shows a worsening of the χ^2/N_{df} when the low- Q^2 data points are included (Fig. 2 left). Apart from missing N³LO contribution, it can be seen as a consequence of missing

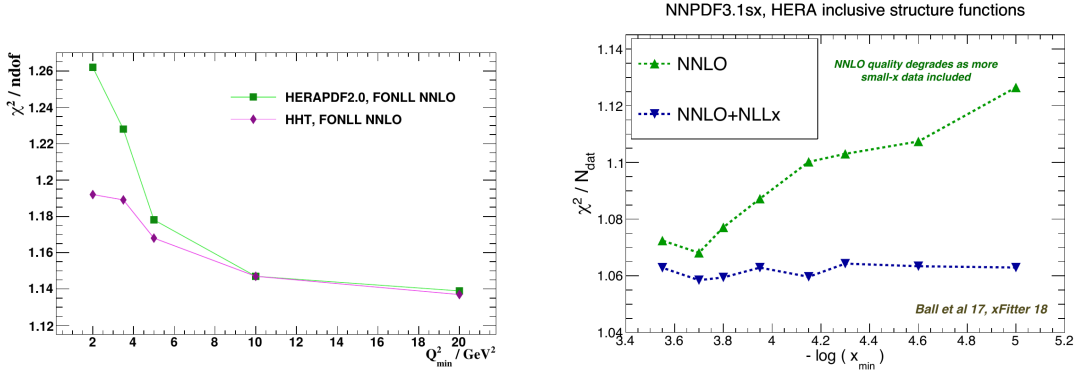


Figure 2: A dependence of the χ^2/N_{df} value on Q_{min}^2 (left) and x_{min} (right), where by definition only the data points with $Q^2(x)$ above the limit are fitted. In the left plot, also the χ^2/N_{df} for model including higher twist effects is shown [7], whereas the right plot shows also χ^2/N_{df} for model incorporating low- x resummation [8].

higher twist effects [7], where apparently the inclusions of these effects improves the χ^2 for low Q_{min}^2 (Fig. 2).

On the other hand, since the inclusion of the low- Q^2 points also means going lower in x , the χ^2 worsening can be related to missing BFKL effects in the theoretical framework. This was studied in detail in [8], where the NNLO DGLAP evolution was supplemented by NLL small- x resummation. The Fig. 2 really demonstrates, that inclusion of the BFKL dynamics improves the data/theory agreement in the low- x region.

The HERA DIS σ_r was extracted up to $x = 6 \times 10^{-7}$, however, the Q^2 for these data points is also very low, and the data are in the non-perturbative region [9] and exhibit a Regge-like behaviour. To reach such x values in the pQCD regime higher beam energies are needed as in the future LHeC [10].

3. Exclusive production of di-photons

The central exclusive production (CEP) $p + p \rightarrow p + X + p$ or $A + A \rightarrow A + X + A$ provides a unique opportunity to study the system X in the clean environment with low particle multiplicity

in the detector. The produced system X can be a pair of jets, pair of photons, pair of W bosons or for example Higgs boson (not measured yet), for a detailed review see [11]. Experimentally, the measurement of these processes is much easier if the forward protons are detected in the forward spectrometers as in AFP [12] at ATLAS or CT-PPS [13] at CMS, since then the momenta of all particles are reconstructed. This can be explicitly checked using energy-momentum conservation.

From the theoretical point of view, there are several mechanisms of such exclusive production.

For example di-photons observed in the detector can originate from QED "light-by-light" scattering diagram (Fig. 3 left) or from QCD-driven diagram (Fig. 3 right). Moreover, in the detector

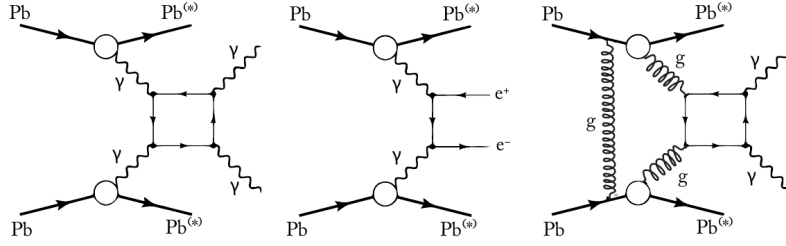


Figure 3: Processes contributing to the exclusive di-photon production in pp or PbPb collisions [14]. The left diagram represents a QED production mechanism, the right diagram QCD-like production. In the detector electrons and/or positrons may be sometime misidentified as photons (middle diagram). In all cases, the incoming protons or nuclei can stay intact or dissociate.

electrons can be misidentified as photons, which represents an extra background to be considered.

The exclusive $\gamma\gamma$ production in pp was measured at Tevatron [15] and the observed cross section was fully consistent with the QCD predictions [16], whereas the QED-like component is predicted to be negligible. Such cross section is roughly proportional to $g(x)^4$, where $x \sim 10^{-3}$, and is therefore very sensitive to the low- x gluon densities.

The QED-like production channel can be enhanced by a factor of $Z^4 \sim 10^7$ if Pb nuclei are collided rather than protons. This was really done at LHC by both ATLAS [17] and CMS [14] collaborations.

The azimuthal decorrelation of the produced photons in CEP is shown in Fig. 4 for both pp and PbPb collisions. In case of the QED production mode, the photons are more back-to-back since the final state protons have lower transverse momenta. The signal peak from "light-by-light" scattering is clearly visible for PbPb, but missing for pp collisions.

In the time of writing, the only existing measurement of the di-photon exclusive production in pp is from Tevatron, and there is no LHC result yet.

4. The forward/backwards jet production at LHC in pp/pA collisions

A forward jet production at LHC allows probing partonic dynamics in the low- x region. The forward dijet system originates from the interaction of the low- x and high- x parton. An imbalance in the momenta of the interacting partons results in a forward boost of the produced jets. Notably, it is interesting to study the pA collisions with A probed at the low- x since the saturation effects in the heavy ions occur at higher x values compared to the proton.

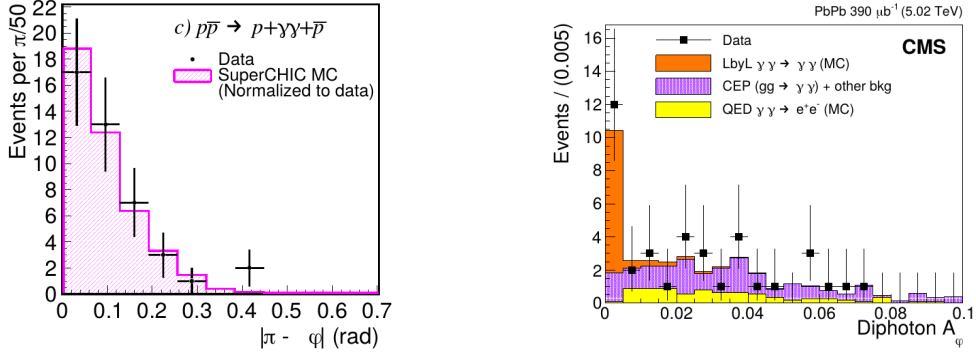


Figure 4: An exclusive diphoton cross section as a function of $\pi - \Delta\Phi$ or $A_\phi = 1 - \frac{\Delta\phi}{\pi}$ as measured at Tevatron in pp collisions [15] (left) or in PbPb collisions at LHC by CMS [14] (right). The predictions for the CMS measurement are divided into several contributions which are explained in Fig. 3, whereas Tevatron data are compared only to the QCD CEP predictions.

In the Fig. 5 (left) the energy spectrum of the forward jets as measured in the CASTOR CMS calorimeter is shown. The forward jets are measured in the direction of the proton beam and

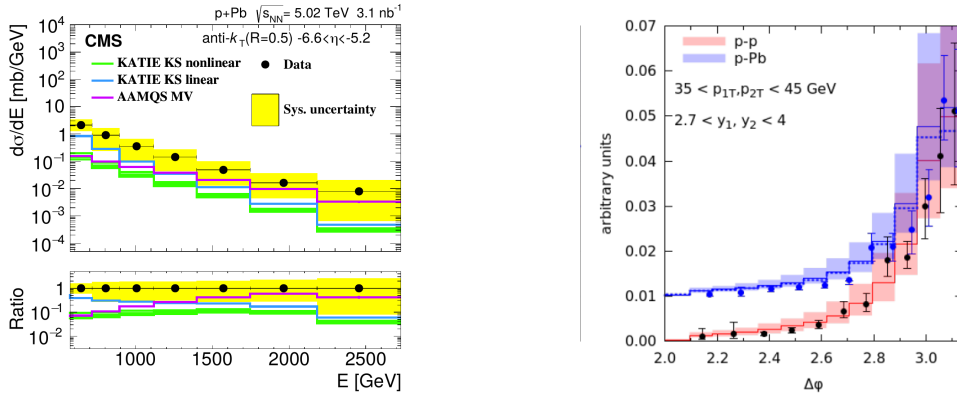


Figure 5: An energy spectrum of jets measured in the forward region by the CASTOR detector at CMS [18] in the pPb collisions (left) and the azimuthal asymmetry of the two forward jets measured by ATLAS in pp/pPb [19] accomplished by predictions from [20] (right). Here for the pPb curves a constant 0.01 was added.

therefore proton is probed at high- x and Pb at low- x . It is apparent that none of the models can describe the data well both in shape and normalization. However, there is an indication that the KaTie-based predictions [21] with KS gluon [22] describe the shape better if the non-linear term is added, i.e. the saturation is included. The forward jets in pp and pPb were also studied by ATLAS (Fig. 5 right), where the angular decorrelation of the two leading jets produced in the forward region was measured. In the ITMD factorization framework [20] observed $\Delta\phi$ broadening in pPb collisions comes from an interplay of the non-linear evolution of the initial state and the Sudakov resummation.

Effects related to the BFKL dynamics can also be studied in forward-backwards jet topologies (so-called Mueller-Navelet jets). Measuring jets in a wide range of rapidity allows for rapidity ordering of the emissions, which is characteristic for parton shower driven by BFKL evolution.

A relevant variable is the azimuthal decorrelation between forward and backward jet, or more precisely a ratio between C_2 and C_1 correlation coefficients, defined as:

$$C_n = \langle \cos n(\pi - \Delta\phi) \rangle. \quad (4.1)$$

The C_2/C_1 ratio as a function of the rapidity difference Δy between jets was measured by both CMS [23] and ATLAS [24] collaborations (Fig. 6). The transverse momenta of the jets are required to be

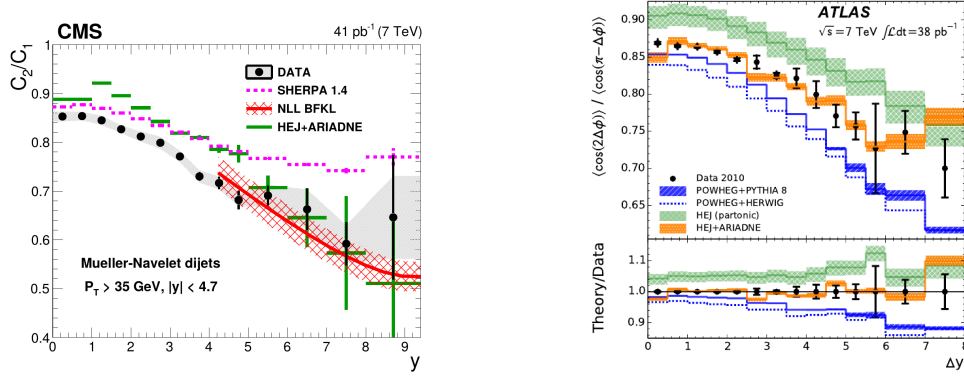


Figure 6: A ratio C_2/C_1 plotted as a function of the rapidity separation Δy between the dijet system as measured by CMS [23] (left) and ATLAS [24] (right). Lower C_2/C_1 corresponds to higher decorrelation of the azimuthal angles of the jets.

above 35 GeV (20 GeV) for CMS (ATLAS) measurement. As expected, LL BFKL (HEJ) or NLL BFKL predictions reasonable describe C_2/C_1 in the high Δy region, where the BFKL dynamics should play a role, whereas classical MC models like SHERPA or POWHEG+Py8 deviate from data.

For the future a high-statistic 13 TeV measurement with asymmetric p_T cuts on jets¹ would be very beneficial to improve our understanding of this process further.

5. Conclusion

In this text we presented a small selection of measurement sensitive to the parton dynamics in the low- x region. Unfortunately, due to limited space, many topics were omitted, for example, diffractive processes or photoproduction of vector mesons. The LHC data improved our understanding of the low- x region a lot, however many processes were measured only at centre-of-mass energy of 7 TeV and the 13 TeV data have not been analyzed yet. In the future, forward proton spectrometers with time detectors should allow measuring exclusive or diffractive processes during standard LHC operation, i.e. in the high pile-up environment. A baseline for any PDF studies still represent the HERA DIS data, and the proposed LHeC collider would extend the phase-space coverage even to lower x values. An Electron Ion Collider (EIC) would bring another vital input, especially to our understanding of the gluon saturation.

¹To ensure the infra-red stability of the NLL BFKL calculations.

From the theory side, it is crucial to improve the precision of predictions for low- x processes. They are often made only at the LO pQCD, where the scale uncertainties are enormous. Furthermore, progress in the low- x MC generators is needed, especially in the simulation of the parton-shower consistent with the low- x evolution equation of the used PDFs.

References

- [1] K. Kutak, *On High Energy Factorization: Theoretical Basics and Phenomenological Applications*, *Acta Phys. Polon.* **B42** (2011) 1487 [1105.0096].
- [2] L. V. Gribov, E. M. Levin and M. G. Ryskin, *Semihard Processes in QCD*, *Phys. Rept.* **100** (1983) 1.
- [3] I. Balitsky, *Operator expansion for high-energy scattering*, *Nucl. Phys.* **B463** (1996) 99 [hep-ph/9509348].
- [4] Y. V. Kovchegov, *Unitarization of the BFKL pomeron on a nucleus*, *Phys. Rev.* **D61** (2000) 074018 [hep-ph/9905214].
- [5] NNPDF collaboration, *Parton distributions from high-precision collider data*, *Eur. Phys. J.* **C77** (2017) 663 [1706.00428].
- [6] H1, ZEUS collaboration, *Combination of measurements of inclusive deep inelastic $e^\pm p$ scattering cross sections and QCD analysis of HERA data*, *Eur. Phys. J.* **C75** (2015) 580 [1506.06042].
- [7] I. Abt, A. M. Cooper-Sarkar, B. Foster, V. Myronenko, K. Wichmann and M. Wing, *Study of HERA ep data at low Q^2 and low x_{Bj} and the need for higher-twist corrections to standard perturbative QCD fits*, *Phys. Rev.* **D94** (2016) 034032 [1604.02299].
- [8] R. D. Ball, V. Bertone, M. Bonvini, S. Marzani, J. Rojo and L. Rottoli, *Parton distributions with small- x resummation: evidence for BFKL dynamics in HERA data*, *Eur. Phys. J.* **C78** (2018) 321 [1710.05935].
- [9] I. Abt, A. M. Cooper-Sarkar, B. Foster, V. Myronenko, K. Wichmann and M. Wing, *Investigation into the limits of perturbation theory at low Q^2 using HERA deep inelastic scattering data*, *Phys. Rev.* **D96** (2017) 014001 [1704.03187].
- [10] R. Abdul Khalek, S. Bailey, J. Gao, L. Harland-Lang and J. Rojo, *Probing Proton Structure at the Large Hadron electron Collider*, *SciPost Phys.* **7** (2019) 051 [1906.10127].
- [11] V. A. Khoze, A. D. Martin and M. G. Ryskin, *Prospects for new physics observations in diffractive processes at the LHC and Tevatron*, *Eur. Phys. J.* **C23** (2002) 311 [hep-ph/0111078].
- [12] L. Adamczyk et al., *Technical Design Report for the ATLAS Forward Proton Detector*, .
- [13] CMS, TOTEM collaboration, *CMS-TOTEM Precision Proton Spectrometer*, .
- [14] CMS collaboration, *Evidence for light-by-light scattering and searches for axion-like particles in ultraperipheral PbPb collisions at $\sqrt{s_{NN}} = 5.02$ TeV*, *Phys. Lett.* **B797** (2019) 134826 [1810.04602].
- [15] CDF collaboration, *Observation of Exclusive Gamma Gamma Production in $p\bar{p}$ Collisions at $\sqrt{s} = 1.96$ TeV*, *Phys. Rev. Lett.* **108** (2012) 081801 [1112.0858].
- [16] L. A. Harland-Lang, V. A. Khoze, M. G. Ryskin and W. J. Stirling, *Standard candle central exclusive processes at the Tevatron and LHC*, *Eur. Phys. J.* **C69** (2010) 179 [1005.0695].

- [17] ATLAS collaboration, *Observation of light-by-light scattering in ultraperipheral Pb+Pb collisions with the ATLAS detector*, *Phys. Rev. Lett.* **123** (2019) 052001 [1904.03536].
- [18] CMS collaboration, *Measurement of inclusive very forward jet cross sections in proton-lead collisions at $\sqrt{s_{NN}} = 5.02$ TeV*, *JHEP* **05** (2019) 043 [1812.01691].
- [19] ATLAS collaboration, *Dijet azimuthal correlations and conditional yields in pp and p+Pb collisions at $s_{NN}=5.02$ TeV with the ATLAS detector*, *Phys. Rev.* **C100** (2019) 034903 [1901.10440].
- [20] A. van Hameren, P. Kotko, K. Kutak and S. Sapeta, *Broadening and saturation effects in dijet azimuthal correlations in p-p and p-Pb collisions at $\sqrt{s} = 5.02$ TeV*, *Phys. Lett.* **B795** (2019) 511 [1903.01361].
- [21] A. van Hameren, *KaTie : For parton-level event generation with k_T -dependent initial states*, *Comput. Phys. Commun.* **224** (2018) 371 [1611.00680].
- [22] K. Kutak and S. Sapeta, *Gluon saturation in dijet production in p-Pb collisions at Large Hadron Collider*, *Phys. Rev.* **D86** (2012) 094043 [1205.5035].
- [23] CMS collaboration, *Azimuthal decorrelation of jets widely separated in rapidity in pp collisions at $\sqrt{s} = 7$ TeV*, *JHEP* **08** (2016) 139 [1601.06713].
- [24] ATLAS collaboration, *Measurements of jet vetoes and azimuthal decorrelations in dijet events produced in pp collisions at $\sqrt{s} = 7$ TeV using the ATLAS detector*, *Eur. Phys. J.* **C74** (2014) 3117 [1407.5756].